Science of the Total Environment 502 (2015) 578–584

Contents lists available at ScienceDirect

Science of the Total Environment

journal homepage: www.elsevier.com/locate/scitotenv

# Effects of meteorology and secondary particle formation on visibility during heavy haze events in Beijing, China

Qiang Zhang [a], Jiannong Quan [a], Xuexi Tie [b,c,*], Xia Li [a], Quan Liu [a], Yang Gao [a], Delong Zhao [a]

[a] Beijing Weather Modification Office, Beijing, China
[b] SKLLQG and Key Laboratory of Aerosol Chemistry and Physics, Institute of Earth Environment, Chinese Academy of Sciences, Xian China
[c] National Center for Atmospheric Research, Boulder, CO, USA

## HIGHLIGHTS

- The cases of haze formation in Beijing, China were analyzed.
- The effects of RH on PM2.5 concentration and visibility were studied.
- Gas-phase to particle-phase conversion under different visibility was analyzed.
- With high RH, the conversion SO2 to SO4= accounted for 20%.

## ARTICLE INFO

*Article history:*
Received 25 July 2014
Received in revised form 5 September 2014
Accepted 24 September 2014
Available online xxxx

Editor: P. Kassomenos

*Keywords:*
Beijing Hazes
Visibility
$PM_{2.5}$
PBL
Secondary particle formation

## ABSTRACT

The causes of haze formation in Beijing, China were analyzed based on a comprehensive measurement, including PBL (planetary boundary layer), aerosol composition and concentrations, and several important meteorological parameters such as visibility, RH (relative humidity), and wind speed/direction. The measurement was conducted in an urban location from Nov. 16, 2012 to Jan. 15, 2013. During the period, the visibility varied from >20 km to less than a kilometer, with a minimum visibility of 667 m, causing 16 haze occurrences. During the haze occurrences, the wind speeds were less than 1 m/s, and the concentrations of $PM_{2.5}$ (particle matter with radius less than 2.5 μm) were often exceeded 200 μg/m$^3$. The correlation between $PM_{2.5}$ concentration and visibility under different RH values shows that visibility was exponentially decreased with the increase of $PM_{2.5}$ concentrations when RH was less than 80%. However, when RH was higher than 80%, the relationship was no longer to follow the exponentially decreasing trend, and the visibility maintained in very low values, even with low $PM_{2.5}$ concentrations. Under this condition, the hygroscopic growth of particles played important roles, and a large amount of water vapor acted as particle matter (PM) for the reduction of visibility. The variations of meteorological parameters (RH, PBL heights, and WS (wind speed)), chemical species in gas-phase (CO, $O_3$, $SO_2$, and NOx), and gas-phase to particle-phase conversions under different visibility ranges were analyzed. The results show that from high visibility (>20 km) to low visibility (<2 km), the averaged PBL decreased from 1.24 km to 0.53 km; wind speeds reduced from 1 m/s to 0.5 m/s; and CO increased from 0.5 ppmv to 4.0 ppmv, suggesting that weaker transport/diffusion caused the haze occurrences. This study also found that the formation of SPM (secondary particle matter) was accelerated in the haze events. The conversions between $SO_2$ and $SO_4^{=}$ as well as NOx to $NO_3^-$ increased, especially under high humidity conditions. When the averaged RH was 70%, the conversions between $SO_2$ and $SO_4^{=}$ accounted for about 20% concentration of $PM_{2.5}$, indicating that formation of secondary particle matter had important contribution for the haze occurrences in Beijing.



## 1. Introduction

High occurrence of haze events (visibility lower than 10 km) in Beijing, the capital city of China, causes deeply concern in the scientific community in recent years. This severe environmental problem has widely impacts on the people's life, traffic, climate, and other important aspects (Charlson et al., 1987; Ramanathan and Vogelmann, 1997; Tegen et al., 2000; Yu et al., 2002; Tie et al., 2009a,b). In haze events, the concentrations of $PM_{2.5}$ (the particle matters with the radius less or equal to 2.5 μm) rapidly increased, with a maximum of 600 μg/m$^3$ (Quan et al., 2013). The extremely high aerosol concentrations caused a very low visibility, and the hygroscopic growth of aerosol particles due to increased RH (relative humidity) in haze events led to further

* Corresponding author at: National Center for Atmospheric Research, Boulder, CO, USA.
*E-mail address:* xxtie@ucar.edu (X. Tie).

http://dx.doi.org/10.1016/j.scitotenv.2014.09.079
0048-9697/

increase their effects on atmospheric visibility (Liu et al., 2011; Quan et al., 2011).

The aerosol concentrations in atmosphere are affected by several factors, including pollutant emissions, atmospheric advection/diffusion, and second aerosol formation etc. (He et al., 2001; Yang et al., 2011; Sun et al., 2013). Large pollutant emission in north China plain (NCP) is a dominant reason for causing the high aerosol concentrations in this region (Tie et al., 2006; Guinot et al., 2007; Chan and Yao, 2008), and unfavorable meteorological conditions can further increase aerosol concentrations. First, there is generally a barrier (very low mixing rate) at the top of the PBL to prevent particles being across from the PBL to the free troposphere (Han et al., 2009; Zhang et al., 2009). As a result, aerosol particles are constrained in the PBL, and aerosol concentrations are anti-correlated with the PBL heights (Zhang et al., 2009; Quan et al., 2013). Second, the aerosol particles are horizontally transported from source regions to downwind regions, and the rate of the transport depends strongly upon wind speeds. In addition to the factors of emission/transport/diffusion, the formation of aerosols might be enhanced due to the participation of liquid phase reactions (Zhang et al., 2013), especially for inorganic components (sulfate, nitrate, ammonia, etc.).

In this work, a comprehensive measurement was carried out during a period (with 16 haze occurrences) from Nov. 16, 2012 to Jan. 15, 2013 to investigate the causes of the occurrences of the haze events. The framework of this study as the following orders; (1) The instruments and measurements were described; (2) The analysis of the results was given. The analysis focuses on the following issues: (a) the characteristics of the haze events, (b) the effects RH on visibility, (c) the relationship between visibility and meteorological and particle conditions, (d) the relative contributions of meteorological and particle conditions to visibility, and (e) the relative contributions of particle composition to visibility in the haze events.

## 2. Instruments and measurements

A comprehensive measurement was conducted from Nov. 16, 2012 to Jan. 15, 2013 in Beijing located at Baolian (BL) meteorological station, China Meteorological Administration (CMA) (39°56′N, 116°17′E). In the measurement, atmospheric visibility, mass concentration of $PM_{2.5}$, chemical composition of non-refractory submicron particles (NR-$PM_1$), gaseous pollutants ($SO_2$, NOx, carbon monoxide (CO), ozone ($O_3$)), and meteorological variables (such as temperature, PBL heights, RH, pressure, wind speed, and wind direction) were observed simultaneously.

The mass concentration of $PM_{2.5}$ was observed by a R&P model 1400a Tapered Element Oscillating Microbalance (TEOM, Thermo Scientific Co., USA) instrument with a 2.5 μm cyclone inlet. The collocated gaseous species including CO, $SO_2$, NOx and $O_3$ were observed by various gas analyzer (Thermo Scientific Co., USA).

Chemical composition of NR-$PM_1$ was measured by an Aerodyne high-resolution Time-of-Flight Aerosol Mass Spectrometer (HR-ToF-AMS). The sampling time resolution was 2 min. The measured composition of particles included sulfate ($SO_4^{=}$), nitrate ($NO_3^-$), ammonium ($NH_4$), chloride (Chl), three primary organic (OA) aerosols, including hydrocarbon-like OA (HOA), cooking OA (COA), and coal combustion OA (CCOA), and one secondary OA aerosol, i.e., oxygenated OA (OOA). According to their origin, PM can be defined into two classes: primary PM (PPM), including, Chl, HOA, COA, CCOA, and secondary PM (SPM), including $SO_4^{=}$, $NO_3^-$, $NH_4$, and OOA.

The evolution of PBL was observed by a micro-pulse lidar (MPL-4B, Sigmaspace Co., USA). Atmospheric visibility was observed by a PWD20 (Vaisala Co., Finland), and meteorology variables were observed by WXT-510 (Vaisala Co., Finland). Detailed instructions of above instruments were given by Quan et al. (2013).

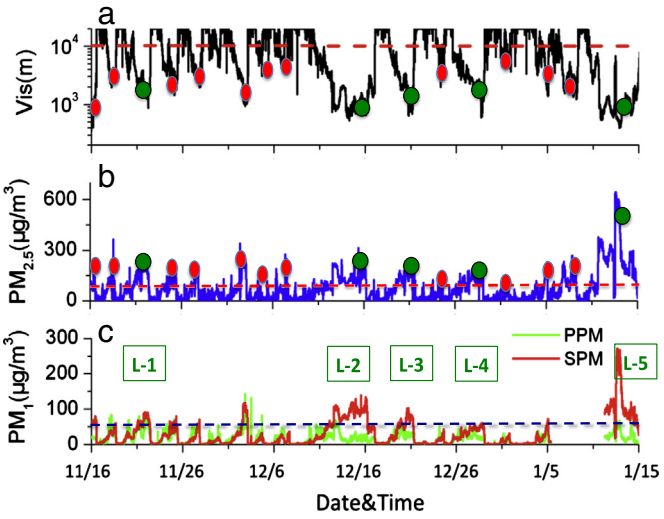


**Fig. 1.** The measured visibility (a), $PM_{2.5}$ concentrations (b), and $PM_1$ (c) from Nov. 16, 2012 to Jan. 15, 2013 at Baolian station in Beijing. There were 16 haze occurrences during this period. The red dots show short-haze events (1–2 days). The blue dots show long-haze events (longer than 3 days), which were also indicated by L-1 to L-5 in panel c. In panel c, the green line presents for PPM and red line for SPM. (For interpretation of the references to color in this figure legend, the reader is referred to the web version of this article.)

## 3. Result and analysis

### 3.1. Characteristics of haze events

According to the definition by CMA (Chinese Meteorological Administration), a haze event is defined by the following conditions, i.e., visibility < 10 km and RH < 90%. During the 2 month experiment period (from Nov. 16, 2012 to Jan. 15, 2013), there were totally 16 haze events, indicating by the red and green dots (see Fig. 1). The time of haze events comprised approximately 60% of the total time in the 2 months, indicating that during wintertime in Beijing, the haze events were very active. During the 16 haze events, the $PM_{2.5}$ concentrations were higher than 100 μg/m$^3$ (see panel b in Fig. 1), suggesting that the high particle concentration was a main reason for causing the haze events. Considering the CMA definition and the measured results, the haze and heavy haze events were clarified in this study as average concentration of $PM_{2.5}$ is above 75 μg/m$^3$ and visibility is less than 5 km for more than 6 h, and average concentration of $PM_{2.5}$ is above 150 μg/m$^3$ and visibility is less than 2 km for more than 12 h, respectively. In addition to this general conclusion, more detailed feathers of the haze events were found, including: (1) The duration of haze events ranged from 1 to 2 days ("short haze" marked by red dots) to 3–6 days ("long haze" marked by green dots). (2) During the "long haze" events, the $PM_{2.5}$ concentrations were extremely high, causing the occurrences of heavy haze (visibility < 1 km). For example, on Jan. 13, 2013, the $PM_{2.5}$ concentrations reached to a maximum value of 600 μg/m$^3$, resulting in a very poor visibility condition (a few hundred meters). (3) The formation of the haze events was in an accumulation mode, especially for the "long haze" events. This feather was clearly indicated during the "long haze" period from Dec. 11 to 16, 2012. During the period, the $PM_{2.5}$ concentration gradually increased from 50 μg/m$^3$ to 200 μg/m$^3$ in 5 days. (4) In contrast to the accumulation mode of the haze formation, the disappearance of the haze events was generally in a quick mode. For example, on Dec. 15, 2012, the $PM_{2.5}$ concentration was about 300 μg/m$^3$ and the visibility was about 1 km. On the next 2 days (Dec. 16–17, 2012), the $PM_{2.5}$ concentration decreased to a small value, and the visibility increased to about 20 km. (5) The secondary particles (SPM) had important contribution to the haze events, especially during the "long haze" events. Fig. 1 (panel c) shows that the measured primary particles (PPM) had a similar magnitude in concentrations compared to the

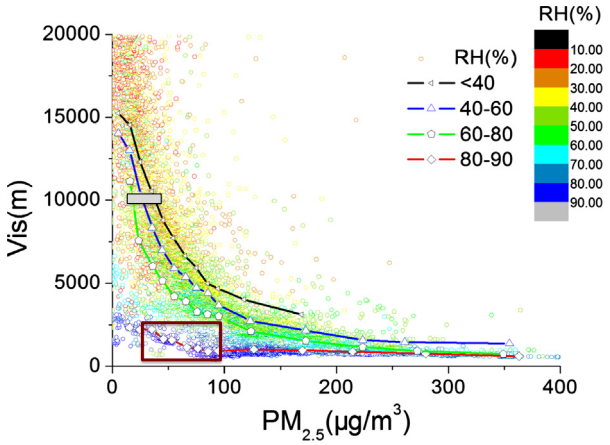


**Fig. 2.** The relationship between the measured visibility and $PM_{2.5}$ concentration under the different RH conditions. The black, blue, green, and red lines present the fits of the dots for the different RH conditions. The dark-red box shows the low visibility with low particle concentration when the RH values were larger than 80%. (For interpretation of the references to color in this figure legend, the reader is referred to the web version of this article.)

secondary concentrations (SPM) during the "short haze" events. However, during the "long haze" events (L-1 to L-5), the PPM concentrations were clearly smaller than the secondary particle concentrations, especially in the late stage of the events. For example, during the early stage of L-2 the PPM and SPM were about 50 μg/m$^3$ on Dec. 12, while during the late sage of L-2, the PPM decreased to about 20 μg/m$^3$, and SPM increased to about 110 μg/m$^3$ on Dec. 16.

### 3.2. Effect of relative humidity on visibility

In addition to aerosol concentration, relative humidity (RH) is also one important factor that affects atmospheric visibility. One of the reasons is that the aerosol composition in Beijing contained a large amount of hydrophilic aerosol particles, such as ammonium sulfate and ammonium nitrate (Sun et al., 2013). These hydrophilic aerosol particles have a strong hygroscopic property, and the radius of aerosol particles can be doubled by coating with the water vapor on the surface of aerosol particles under high RH value (>80%) (Liu et al., 2011). Fig. 2 shows the relationship between visibility and $PM_{2.5}$ concentrations under the different RH conditions. With the increase of $PM_{2.5}$ concentration, the visibility range decreased correspondingly, but their relation appears in a non-linearity correlation. When $PM_{2.5}$ concentrations were very high (above 100 μg/m$^3$), the change in visibility was not sensitive to $PM_{2.5}$ concentration. In contrast, when aerosol concentrations were low (under 100 μg/m$^3$), the change in visibility was very sensitive to aerosol concentrations. For example, with RH of 40–60%, when aerosol concentration increased from 100 μg/m$^3$ to 200 μg/m$^3$, visibility decreased from 3.7 km to 2.5 km. The ratio of the changes between visibility and $PM_{2.5}$ ($\Delta Vis/\Delta PM_{2.5}$) was −0.012 (km μg$^{-1}$ m$^3$). In contrast, when aerosol concentration increased from 50 μg/m$^3$ to 100 μg/m$^3$, visibility decreased from 6.5 km to 3.0 km. The ratio of ($\Delta Vis/\Delta PM_{2.5}$) is −0.070 (km μg$^{-1}$ m$^3$), which is about 6 times higher than the first value.

It is worth to note that when RH value was below 80%, the relationships between $PM_{2.5}$ concentration and visibility were in a similar matter (an exponentially decreasing trend), with a tendency toward lower visibility from the lower RH range (<40%) to the higher RH range (60–80%). There was also a threshold concentration (50 μg/m$^3$) of $PM_{2.5}$. Under the threshold concentration, the visibility was above 10 km, which was in a non-haze condition, while above the threshold concentration, the visibility was less than 10 km, which was in a haze condition. According to the previous studies, the threshold concentrations were found to range from 80 μg/m$^3$ to 100 μg/m$^3$ in Guangzhou (Deng et al., 2008) and in Xi'an (Cao et al., 2012). These values are higher than the value in Beijing due to the different characteristics of particles (size distributions, composition of particles, etc.).

Fig. 2 also shows that when the RH values were very high and above 80% (80–90%), the relationship between $PM_{2.5}$ concentration and visibility was very different with the low RH cases. First, the relationship was no longer to follow the exponentially decreasing trend. Second, the visibility kept in a very low value, even with low $PM_{2.5}$ concentrations. For example, when $PM_{2.5}$ concentrations ranged between 25 μg/m$^3$ and 100 μg/m$^3$, the visibilities changed from 2.5 km to 1.0 km, respectively. In contrast, the visibilities changed from 7.5 km to 3.0 km, with RH of 60–80%. This result suggests that there was a rapid hygroscopic growth of particles, especially in the case of RH > 80%. In this case, a large amount of water vapor coated on particle surface, and acted as scattering particles to significantly reduce visibility. Using the measured results, the amount of water coating on particle surface can be estimated. For the visibility of 2.5 km, the averaged concentrations of $PM_{2.5}$ were 25 μg/m$^3$ and 150 μg/m$^3$ for RH of 80–90% and 40–60%, respectively. If the numbers of particles were not changed, the mass of particles increased by 6 times, implying that the size of particles increased by approximate 2.5 times.

### 3.3. Relationship of visibility with meteorology and particles

In order to get more insights of the development of haze events in this region, the relationships between visibility and the meteorological parameters (RH, PBL height, and wind speed), chemical species in gas-phase (CO, $O_3$, $SO_2$, and NOx), particles ($PM_{2.5}$ and $PM_1$) were analyzed. Based on the ranges of visibility, the visibility was classified into 4 categories: (a) visibility > 10 km (V1) which presents the non-haze days following the definition of CMA; (b) 10 km ≥ visibility >5 km (V2) which presents light haze days; (c) 5 km ≥ visibility > 2 km (V3) which present modest-heavy haze days; and (d) 2 km ≥ visibility (V4) which present extreme haze days. Fig. 3 shows the variations of $PM_{2.5}$, $PM_1$, RH, $PBL_{max}$ (daily maximum PBL height), wind speed, CO, $O_3$, $SO_2$, NOx, the ratios of N (nitrogen) and S (sulfur), under the 4 visibility conditions. The $PBL_{max}$ was defined as the PBL height during 13:00–15:00. The N and S ratios were the ratios between the particle phase of nitrogen and sulfur ($N_a$ and $S_a$) and the total nitrogen and sulfur (both gas and particle phases; $N_a + N_g$ and $S_a + S_g$).

Fig. 3 shows that (1) the particle concentrations ($PM_{2.5}$ and $PM_1$) rapidly increased with the decrease in visibility. The $PM_{2.5}$ concentrations increased from about 10 μg/m$^3$ at V1 to 185 μg/m$^3$ at V4, and the $PM_1$ concentrations increased from about 5 μg/m$^3$ at V1 to 105 μg/m$^3$ at V4, suggesting that the high PM concentrations were the main reason for the poor visibility in Beijing. Previous studies (Quan et al., 2013; Zhang et al., 2013; and He et al., in press) suggested that meteorological parameters, such as PBL height, wind speed, and relative humidity caused a strong variability for PM concentrations, which was consistent with this study. The $PBL_{max}$ decreased with the decrease of visibility (i.e., increase in PM concentrations). The $PBL_{max}$ height was 1.24 km and 0.53 km in V1 and V4 respectively. The lower PBL height depressed particles in a shallower layer, and caused higher PM concentrations and lower visibility. The wind speed during this entire episode was very low (lower than 1 m/s). For example, the averaged wind speed was 1 m/s at V1, and around 0.5 m/s at V2, V3, and V4. The low wind speed was also a main factor to cause the heavy haze frequently occurred during the episode (16 occurrences). Another important meteorological parameter was the relative humidity, and it strongly correlated with the visibility during the episode. The RH values increased with the decrease of visibility. At V1, the averaged RH value was 25%, and at V4, it increased to 70%.

Gas-phase chemical species (CO, $O_3$, $SO_2$, and NOx) were also significantly varied under the different visibility ranges. The concentrations of CO increased with the decrease of visibility. At V1, the CO concentration was about 0.5 ppmv, but it rapidly increased to about 4.0 ppmv at V4. CO is not an active photochemical species, and its chemical lifetime is

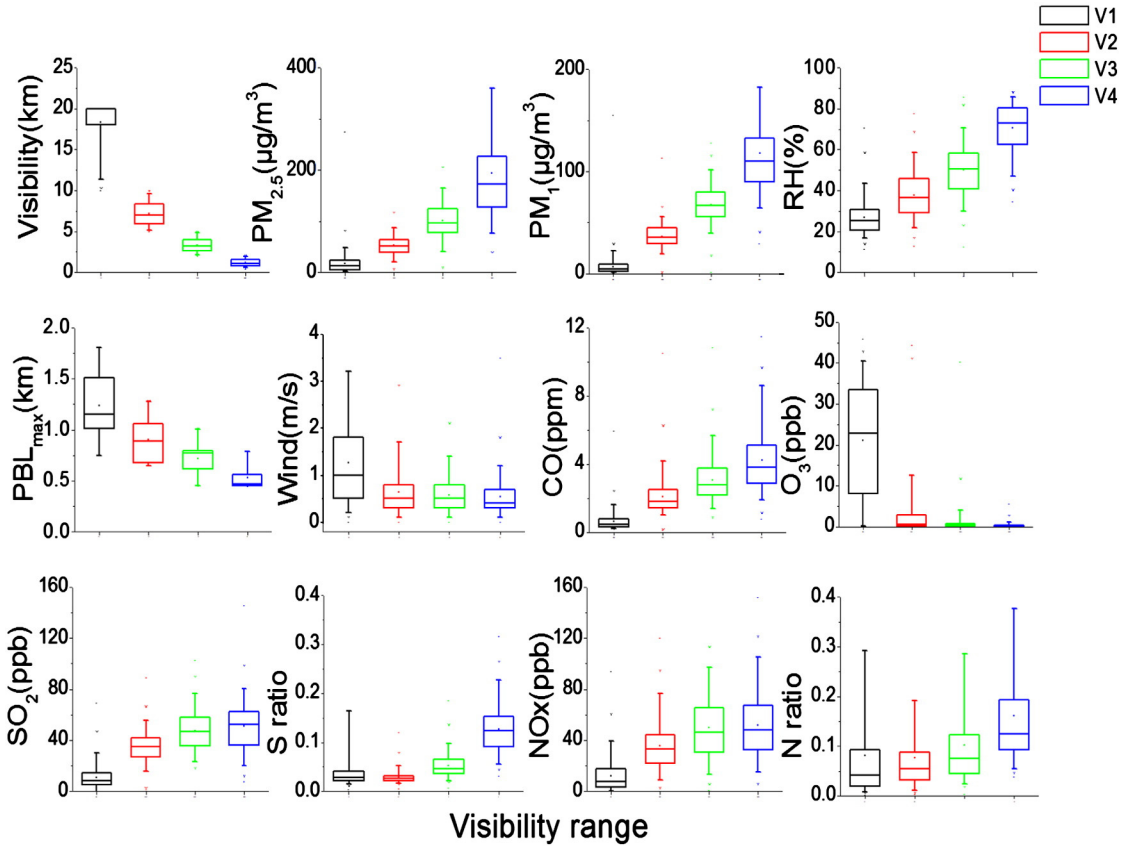


**Fig. 3.** The relationship between the measured visibility and the meteorological parameters (RH, PBL heights, and wind speeds), chemical species in gas-phase (CO, $O_3$, $SO_2$, and NOx), particles ($PM_{2.5}$ and $PM_1$) under the different visibility ranges (V1, V2, V3, and V4).

about a few months. In a short period, CO can be considered as an inert pollution tracer, which was mainly controlled by meteorological parameters (Brasseur et al., 1999; Tie et al., 2013). The correlation between visibility and CO concentration shows that the CO concentration increased with the decrease of visibility. The concentrations of CO were 0.5 ppmv and 3.8 ppmv at V1 and V4, respectively, suggesting that the meteorological conditions (such as lower PBL height and wind speed) played important roles in controlling the air pollutants.

The concentration of $O_3$ decreased when the visibility decreased. Because tropospheric $O_3$ is produced by photochemical processes (Chameides and Walker, 1976), the concentrations are low under weak photochemical activities (low visibility range). It is worth to note that the concentrations of $O_3$ were close to zero under the V2, V3, and V4 conditions. This result suggested that the $O_3$ photochemical production eased during haze events during wintertime in Beijing.

The variations of $SO_2$ and NOx had a similar pattern. The concentrations of $SO_2$ and NOx rapidly increased from V1 to V2. However, the increase of $SO_2$ and NOx was slow from V3 to V4. Because the RH values increased from 50% (V3) to 70% (V4), one explanation for the slow growth is that the gas-phase of $SO_2$ and NOx converted to particle-phase under high humidity conditions (Zhang et al., 2013). This conversion also showed in the S ratio (defined as $S_a/(S_a + S_g)$; $S_a$ represents the sulfur mass in aqueous phase, and $S_g$ represents the sulfur mass in gas phase), and N ratio (defined as $N_a/(N_a + N_g)$; $N_a$ represents the nitrogen mass in aqueous phase, and $N_g$ represents the nitrogen mass in gas phase). The ratios were useful to determining the magnitudes of the gas-phase to aqueous-phase conversions. For example, the higher values of the ratios suggested more aqueous-phase were formed during haze events. Both the ratios had a rapid increase from V3 and V4, especially for the S ratio. It is interesting to note that the changes were small from V1 to V3, with the RH values were less than 50%. This result suggests that chemical conversions from gas-phase ($S_g$ and $N_g$) to particle-phase ($S_a$ and $N_a$) occurred rapidly under high humidity condition.

### 3.4. Meteorological and chemical contributions

Above analysis indicated that both meteorological and chemical processes could influence aerosol concentration in haze events. To estimate the relative contribution of meteorological and chemical processes to the haze events, CO is selected as a chemical inactive tracer because of it's long chemical lifetime. The chemical lifetime of CO ranges about a

**Table 1**
Media values of measured visibility, particles, meteorological parameters, chemical concentrations, and S, N ratios under different visibility ranges (V1, V2, V3, and V4).

| Variables | V1 | V2 | V3 | V4 |
|---|---|---|---|---|
| Visibility (km) | 16.0 | 7.0 | 2.6 | 0.6 |
| $PM_{2.5}$ (μg/m$^3$) | 11 | 52 | 95 | 185 |
| $PM_{1.0}$ (μg/m$^3$) | 5 | 33 | 62 | 105 |
| RH (%)25 | 36 | 50 | 70 | |
| PBL (km) | 1.2 | 0.9 | 0.7 | 0.5 |
| Wind speed (m/s)0.9 | 0.5 | 0.5 | 0.4 | |
| CO (ppmv) | 0.5 | 1.8 | 2.2 | 3.8 |
| $O_3$ (ppbv) | 22.0 | 1.0 | 0.5 | 0.4 |
| $SO_2$ (ppbv) | 8 | 38 | 45 | 50 |
| S_ratio | 0.01 | 0.02 | 0.03 | 0.12 |
| NOx (ppbv) | 4 | 32 | 45 | 50 |
| N_ratio | 0.04 | 0.05 | 0.07 | 0.11 |

Note:
V1 (visibility > 10 km).
V2 (10 km ≥ visibility >5 km).
V3 (5 km ≥ visibility >2 km).
V4 (2 km ≥ visibility).

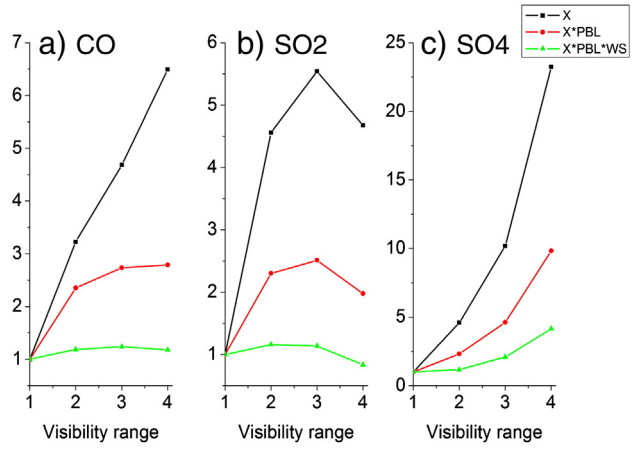


**Fig. 4.** The variations of CO, CO * PBL, and CO * PBL * WS (a), $SO_2$, $SO_2$ * PBL, and $SO_2$ * PBL * WS (b), and $SO_4$, $SO_4$ * PBL, and $SO_4$ * PBL * WS (c) under the different visibility ranges (V1, V2, V3, and V4). The y-axis units are the relative values with the reference values at V1.

few months, which depends upon the concentration of OH value (Brasseur et al., 1999). As a result, the variability of CO is mainly controlled by meteorological factors. As indicated in Fig. 3 (the detailed values are shown in Table 1) with the decreasing in visibility, CO increased. The increase in CO was strongly related to the meteorological factors, such as the decease of the PBL heights and wind speeds. Because the concentration of CO was relatively constrained within PBL based on the vertical measurement aircraft over the north China plain (Liu et al., 2009; Zhang et al., 2009), CO * PBL was calculated under different visibility range. Because the changes of PBL (decreasing from V1 to V4) were already contained in the variable of CO * PBL, the PBL effect was eliminated, and the variation of CO * PBL was mainly affected by wind speed. To further eliminate the effect of wind speed, CO * PBL * WS was also calculated. The values of CO * PBL * WS were useful to compare with the values of $SO_2$ * PBL * WS and $SO_4^{=}$ * PBL * WS. Because CO can be considered as a chemical inert tracer, while $SO_2$ and $SO_4^{=}$ were chemically active. The gas to aqueous phase conversions led to decrease in $SO_2$ and increase in $SO_4^{=}$ (Zhang et al., 2013). If the trends were similar between CO * PBL * WS and $SO_2$ * PBL * WS, it suggested that no significant occurrence of chemical conversions happened between $SO_2$ and $SO_4^{=}$. Otherwise, important chemical conversions were happened. As shown in Fig. 4, the value of CO * PBL increased from V1 to V4, but the increase trend was significantly slower than the trend of CO itself, suggesting that the decrease of PBL height strongly affect the CO concentrations, especially in the visibility ranges of V3 and V4. The value of CO * PBL * WS was close to a constant value, suggesting that the 2 meteorological factors (PBL height and wind speed) were the 2 major factors for affecting the variability of CO under different visibility conditions. In contrast, the value of $SO_2$ * PBL * WS was not a constant, it strongly decreased from V3 to V4, suggesting that the decreasing of $SO_2$ was not due to meteorological processes rather than chemical processes. It is interesting to note that the value of $SO_4^{=}$ * PBL * WS was also not a constant value, it strongly increased from V3 to V4. The decrease of $SO_2$ * PBL * WS and the increase of $SO_4^{=}$ * PBL * WS indicated the chemical conversion from gas-phase ($SO_2$) to particle-phase ($SO_4$) under high humidity condition (70% in V4).

To further understand the relative contribution of the chemical processes to $PM_{2.5}$, $SO_2$, NOx, and $O_3$ in the haze events, the ratios of $PM_{2.5}$/CO, $SO_2$/CO, NOx/CO, and $O_3$/CO were calculated under the different visibility conditions. As we mentioned, CO can be considered as a tracer, and the variability due to meteorological factors was excluded from the ratios. The results show that for the ratio of $PM_{2.5}$/CO, it increased with the decrease of the visibility ranges, indicating that more secondary $PM_{2.5}$ was produced in the lower visibility conditions. For the ratio of $SO_2$/CO, it rapidly decreased with the decrease of the visibility ranges, suggesting that more chemical conversion from gas-phase to particle-phase occurred in the lower visibility condition. For the ratio of NOx/

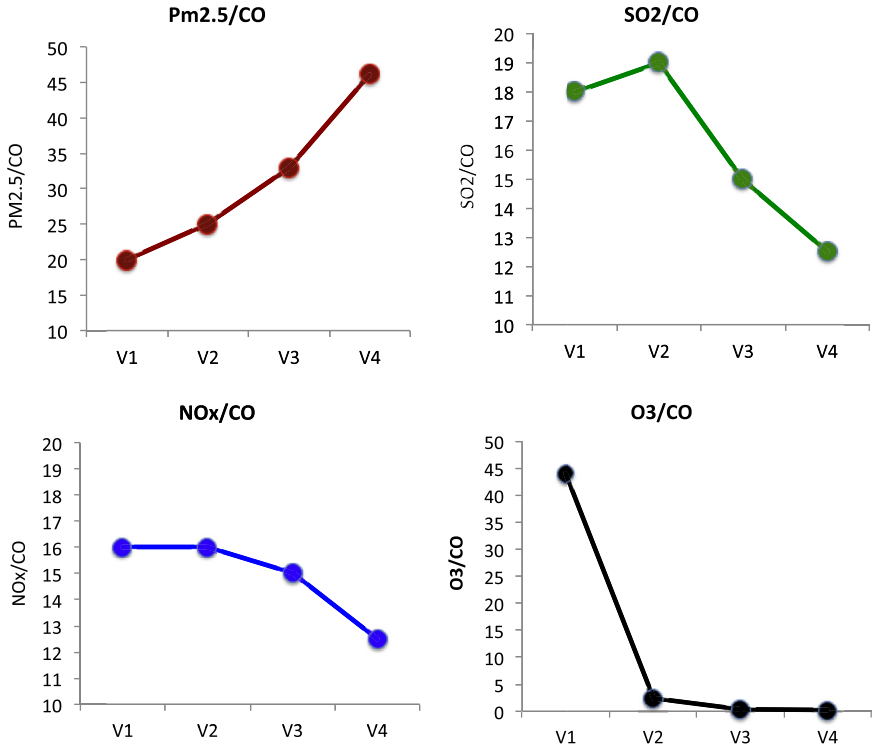


**Fig. 5.** The measured ratios of $PM_{2.5}$/CO (μg/m$^3$/ppmv), $SO_2$/CO (ppbv/ppmv), NOx/CO (ppbv/ppmv), and $O_3$/CO (ppbv/ppmv) under the different visibility ranges (V1, V2, V3, and V4). Because CO is considered as an inert tracer, the changes in the ratios suggest the chemical activities in different visibility conditions.

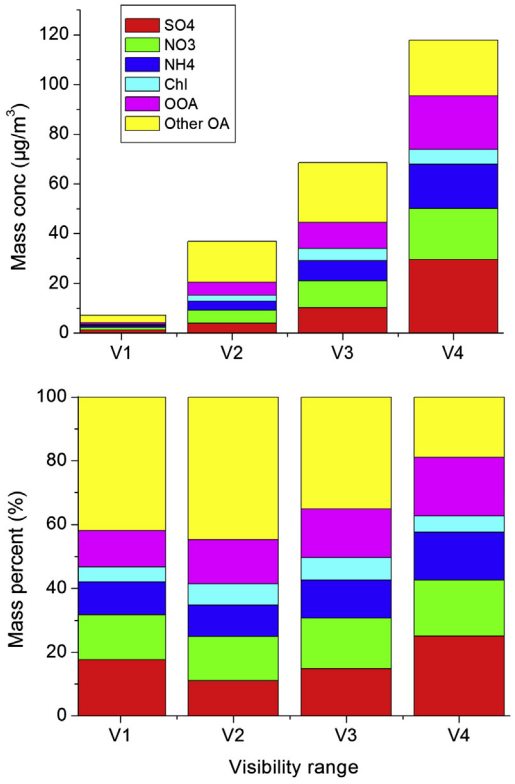


**Fig. 6.** The measured primary particles (PPM), including Chl, HOA, COA, and CCOA, and secondary particles (SPM), including $SO_4^{=}$, $NO_3^{-}$, $NH_4$, and OOA, under the different visibility ranges (V1, V2, V3, and V4). The other OA contains HOA, COA, and CCOA. The upper panel presents the mass concentrations (μg/m$^3$), and the lower panel shows the mass percentage (%).

CO, it also decreased with the decrease of the visibility ranges, but the rate of decrease was slower than the ratio of $SO_2$/CO, suggesting that there was less chemical gas-phase to particle-phase conversion for NOx than $SO_2$, which was consistent to the study by Zhang et al. (2013). Both the result of $SO_2$/CO and NOx/CO ratios was consistent with the result of S ratio and N ratio (shown in Fig. 3). Finally, for the ratio of $O_3$/CO, it rapidly decreased with the decrease of the visibility from V1 to V2, and remained in a very low value in V3 and V4, suggesting that photochemical production of $O_3$ was ceased during the occurrences of haze events, which was also suggested by Bian et al. (2007) (Fig. 5).

### 3.5. Chemical composition in different visibility conditions

The above analysis shows that secondary particle formation was another factor to increase aerosols concentration in haze events. To investigate the evolution of the secondary particle formation, the changes of primary (PPM–Chl, HOA, COA, and CCOA) and secondary (SPM–$SO_4^{=}$, $NO_3^{-}$, $NH_4$, and OOA) under different visibility ranges were shown in Fig. 6.

The upper panel of Fig. 6 shows that mass concentrations of particles under the different ranges of visibility. It shows that the mass concentrations increased rapidly from V1 to V4. The rapid increases include both of the increases of PPM and SPM. The relative increases (increases in percentage) show the information of secondary particle formation in the haze events. As shown in the lower panel of Fig. 6, the percentage of SPM species increased with the decrease in visibility, especially from V2 to V4. For example, $SO_4$ changed from 11% to 25%; $NH_4$ changed from 10% to 15%; $NO_3^{-}$ changed from 14% to 18%; and OOA changed from 14% to 18%. Contrary to the variation of SPM, the percentage of PPM decreased correspondingly. For example, CCOA changed from 15% to 7%; HOA changed from 13% to 8%; COA changed from 7% to 3%; and Chl changed from 7% to 5%. The composition measurements were consistent with the N ratio and S ratio analysis. The most important secondary particle formation was from the gas-phase ($SO_2$) to particle-phase ($SO_4^{=}$) conversion under low visibility with low concentration condition (35 μg/m$^3$ in V4). Compared to the concentration of $PM_{2.5}$ in V4 (175 μg/m$^3$ in V4), it was about 20% increase.

## 4. Summary

A comprehensive measurement was made to investigate the causes of the haze events in Beijing during the winter of 2012–2013. The results are highlighted as follows:

(1) High aerosols and RH are two important factors that cause low visibility events in Beijing. In haze events, the visibility can be rapidly decreased from >20 km to <2 km in 1–2 days due to the increases of $PM_{2.5}$ concentrations and the RH values. The correlation between $PM_{2.5}$ concentration and visibility under different RH value shows that the visibility was exponentially decreased with the increase of $PM_{2.5}$ concentrations when RH was less than 80%. However, when RH was higher than 80%, the relationship was no longer to follow the exponentially decreasing trend, and the visibility maintained in very low values, even with low $PM_{2.5}$ concentrations. Under this condition, the hygroscopic growth played important roles, and a large amount of water acted as particle matter (PM) for the reduction of visibility.

(2) The variations of meteorological parameters (RH, PBL heights, and WS), chemical species in gas-phase (CO, $O_3$, $SO_2$, and NOx), and gas-phase to particle-phase conversions under different visibility ranges were analyzed. The results show that from high visibility (>20 km) to low visibility (<2 km), the averaged PBL decreased from 1.24 km to 0.53 km; wind speeds reduced from 1 m/s to 0.5 m/s; and CO increased from 0.5 ppbv to 4 ppbv, suggesting that the weak transport/diffusion was an important factor to cause the haze occurrences.

(3) The ratios of $PM_{2.5}$/CO, $SO_2$/CO, NOx/CO, and $O_3$/CO were calculated under the different visibility conditions. For the ratio of $PM_{2.5}$/CO, it increased with the decrease of the visibility ranges, indicating that more secondary $PM_{2.5}$ was produced in the lower visibility conditions. For the ratio of $SO_2$/CO, it rapidly decreased with the decrease of the visibility ranges, suggesting that more chemical conversion from gas-phase to particle-phase occurred in the lower visibility condition. For the ratio of NOx/CO, it also decreased with the decrease of the visibility ranges, but the rate of decrease was slower than the ratio of $SO_2$/CO, suggesting that there was less chemical gas-phase to particle-phase conversion for NOx than $SO_2$. Both the result of $SO_2$/CO and NOx/CO ratios suggests that secondary particle formation (SPM) was accelerated in haze events. The conversions between $SO_2$ and $SO_4^{=}$ as well as NOx to $NO_3^{-}$ increased, especially under high humidity conditions. When the averaged RH was 70%, the conversions between $SO_2$ and $SO_4^{=}$ accounted for about 20% concentration of $PM_{2.5}$, indicating that formation of secondary particle matter had important contribution to the haze occurrences in Beijing.

## Acknowledgments

This research is partially supported by the National Natural Science Foundation of China (NSFC) under Grant Nos. 41375135 and 41175007, and the National Basic Research Program of China (2011CB403401). The National Center for Atmoshperic Research is sponsored by the National Science Foundation.

## References


Bian H, Han SQ, Tie X, Shun ML, Liu AX. Evidence of impact of aerosols on surface ozone concentration: a case study in Tianjin, China. Atmos Environ 2007;41:4672–81.

Brasseur GP, Orlando JJ, Tyndall GS. Atmospheric chemistry and global change. New York: Oxford Univ. Press; 1999.

Cao JJ, Wang QY, JC Chow, Watson JG, Tie X, Shen ZX, Wang P, An ZS. Impacts of aerosol compositions on visibility impairment in Xi'an, China. Atmos Environ 2012;59: 559–66. http://dx.doi.org/10.1016/j.atmosenv.2012.05.036.

Chameides WL, Walker J. Time dependent photochemical model for ozone near the ground. J Geophys Res 1976;81:413–20.

Chan CK, Yao X. Air pollution in megacities in China. Atmos Environ 2008;42(1):1–42.

Charlson RJ, Lovelock JE, Andreae MO, Warren SG. Oceanic phytoplankton, atmospheric sulfur, cloud albedo and climate. Nature 1987;326:655–61.

Deng XJ, Tie X, Wu D, Zhou XJ, Tan HB, Li F, et al. Long-term trend of visibility and its characterizations in the Pearl River Delta Region (PRD), China. Atmos Environ 2008;42: 1424–35.

Guinot B, Cachier H, Sciare J, Yu T, Wang X, Yu JH. Beijing aerosol: atmospheric interactions and new trends. J Geophys Res 2007;112(D14314). http://dx.doi.org/10.1029/2006JD008195.

Han SQ, Bian H, Tie X, Xie Y, Sun M, Liu A. Impact measurements of nocturnal planetary boundary layer on urban air pollutants: from a 250-m tower over Tianjin, china. J Hazard Mater 2009;162:264–9.

He KB, Yang F, Ma YL, Zhang Q, Yao XH, Chan CK, et al. The characteristics of PM2.5 in Beijing, China. Atmos Environ 2001;35:4959–70.

He H, Tie X, Zhang Q, Liu X, Gao Q, Li X, et al. Analysis of the causes of heavy aerosol pollution in Beijing, China: A case study with the WRF-Chem model. Particuology 2014. [in press]. http://dx.doi.org/10.1016/j.partic.2014.06.004.

Liu PF, Zhao CS, Zhang Q, Deng ZZ, Huang MY, Ma XC, et al. Aircraft study of aerosol vertical distributions over Beijing and their optical properties. Tellus 2009;61B:756–67.

Liu PF, Zhao CS, Gobel T, Hallbauer E, Nowak A, Ran L, et al. Hygroscopic properties of aerosol particles at high relative humidity and their diurnal variations in the North China Plain. Atmos Chem Phys 2011;11:3479–94.

Quan JN, Zhang Q, Liu JZ, Huang MY, Jin H. Analysis of the formation of fog and haze in North China Plain (NCP). Atmos Chem Phys 2011;11:8205–14.

Quan JN, Gao Y, Zhang Q, Tie X, Cao J, Han S, et al. Evolution of planetary boundary layer under different weather conditions, and its impact on aerosol concentrations. Particuology 2013;11:34–40. http://dx.doi.org/10.1016/j.partic.2012.04.005.

Ramanathan V, Vogelmann AM. Greenhouse effect, atmospheric solar absorption, and the Earth's radiation budget: from the Arrhenius–Lanely era to the 1990s. Ambio 1997; 26(1):38–46.

Sun YL, Wang ZF, Fu PQ, Yang T, Jiang Q, Dong HB, et al. Aerosol composition, sources and processes during wintertime in Beijing, china. Atmos Chem Phys 2013;13:4577–92.

Tegen I, Koch D, Lacis AA, Sato M. Trends in tropospheric aerosol loads and corresponding impact on direct radiative forcing between 1950 and 1990: a model study. J Geophys Res 2000;105:26971–90.

Tie X, Brasseur G, Zhao C, Granier C, Massie S, Qin Y, et al. Chemical characterization of air pollution in Eastern China and the Eastern United States. Atmos Environ 2006;40: 2607–25.

Tie X, Madronich S, Li GH, Ying ZM, Weinheimer A, Apel E, et al. Simulation of Mexico City Plumes during the MIRAGE-Mex Field campaign using the WRF-Chem model. Atmos Chem Phys 2009a;9:4621–38.

Tie X, Wu D, Brasseur G. Lung cancer mortality and exposure to atmospheric aerosol particles in Guangzhou, China. Atmos Environ 2009b;43:2375–7.

Tie X, Geng F, Guenther A, Cao J, Greenberg J, Zhang R, et al. Megacity impacts on regional ozone formation: observations and WRF-Chem modeling for the MIRAGE-Shanghai field campaign. Atmos Chem Phys 2013;13:5655–69. http://dx.doi.org/10.5194/acp-13-5655-2013.

Yang F, Tan J, Zhao Q, Du Z, He K, Ma Y, et al. Characteristics of PM2.5 speciation in representative megacities and across China. Atmos Chem Phys 2011;11:5207–19.

Yu H, Liu SC, Dickinson RE. Radiative effects of aerosols on the evolution of the atmospheric boundary layer. J Geophys Res 2002;107:4142. http://dx.doi.org/10.1029/2001JD000754.

Zhang Q, Ma XC, Tie X, Huang MY, Zhao CS. Vertical distributions of aerosols under different weather conditions; analysis of in-situ aircraft measurements in Beijing, China. Atmos Environ 2009;9:4621–38.

Zhang Q, Tie X, Lin WL, Cao JJ, Quan JN, Ran L, et al. Measured variability of $SO_2$ in an intensive fog event in the NCP region, China; evidence of high solubility of $SO_2$. Particuology 2013:41–7. http://dx.doi.org/10.1016/j.partic.2012.09.005.